# SPatial Atmospheric Cloud Explorer (SPACE)

Jinrong Xie[1] Franz Sauer[2] Hendrik Schroots[3] Chuan Wang[4] Shimin Wang[5] Kwan-Liu Ma[6]
University of California, Davis

## 1 Initial Data Integration and Browsing (Task 1)

Our system, the Spatial Atmospheric Cloud Explorer (SPACE), is designed to aid scientists in studying the global atmospheric effects caused by volcanic eruptions. In this system, we allow users to view the data on either a 3D spherical model of the earth (Figure 1) or a "2D" equirectangular projection (Figure 2) where longitude and latitude represent the x or y coordinates of the image respectively. Mapping altitude information in the z direction can also give the projected view a 3D representation when viewed at certain angles. While the spherical model provides a more realistic view with enhanced 3D structure the projection delivers a better overview of the data distribution in the geospatial domain.

The MIPAS detections are shown in 3D and are represented as point sprites as seen in Figure 2. Different colors are assigned to the points to represent the type of each detection. The CLaMS trajectories are shown as curves in 3D and represent the estimated history of the MIPAS point location through time. An image showing the CLaMS trajectories can be seen in Figure 3. The tail of the trajectory becomes transparent over time so that users can easily distinguish the front of the trajectory. Each curve is also multicolored representing scalar values at that particular point in time. By studying how the color changes along a trajectory, users can gain temporal insight from just a single frame of the animation. As the AIRS dataset has no altitude information, we represent it as a 2D texture projected onto the earth's surface as seen in Figure 4. Color intensity is used to represent the strength of the measured value. Moreover, since the different data modalities all reside in the same geospatial and temporal domain, we can display them in conjunction with one another.

We display temporal variations in each of the datasets as an animation that users can play, pause, and seek through. While the CLaMS trajectories have a more quasi-continuous representation, the MIPAS and AIRS datasets have a lower temporal resolution. For these datasets, we load an appropriate time window (usually 12 hours) in order to match the current time frame while still providing global coverage of the data. The length of the CLaMS curves is then adjusted to match the time window. Users can toggle the rendering of each of the three data modalities separately, significantly reducing the amount of clutter in the visualization. In addition, users can choose to isolate CLaMS trajectories in either the northern or southern hemispheres and adjust the length of the curves by changing the time window size. In order to help users efficiently browse through the data, we implement a number of "bookmarks" at key events, such as the eruption date of each volcano. Users can quickly jump to a particular eruption instead of tediously seeking through less interesting timesteps.

[1] e-mail: jrxie@ucdavis.edu
[2] e-mail: fasauer@ucdavis.edu
[3] e-mail: hschroots@ucdavis.edu
[4] e-mail: vvang@ucdavis.edu
[5] e-mail: wyudun@gmail.com
[6] e-mail: ma@cs.ucdavis.edu

## 2 Linking MIPAS Detections to Eruptions (Task 2)

We associate MIPAS detections with eruption events by utilizing the CLaMS trajectories. Since each trajectory is uniquely seeded at a particular MIPAS point, we can first associate each MIPAS measurement with a CLaMS trajectory, and then use the geospatial information of the CLaMS trajectory to trace each measurement back to an eruption event. This allows us to associate eruption events with CLaMS trajectories, and as a result, the MIPAS measurements as well.

Since all points are given in a common reference frame (latitude, longitude, altitude, time), we are able to match the associated MIPAS measurement for any given seed point of a CLaMS trajectory. We include a reasonable error threshold when building this correspondence to account for any minor discrepancies between the two data modalities. This one-to-one mapping provides an approximation to the historical and future movement of each MIPAS detection. Tracing each MIPAS point through time along its associated CLaMS pathline allows us to generate a continuous visualization of particular ash plumes and can be seen in Figure 5. We employ a cubic hermite spline to better interpolate intermediate positions at arbitrary times on a CLaMS curve.

In the southern hemisphere, it is easy to associate detections to the single eruption event. However, care must be taken to separate detections in the northern hemisphere from the Grimsvotn and Nabro eruptions. We do this by identifying AIRS $SO_2$ detections within a predefined perimeter around the Nabro volcano. We then search and tag CLaMS pathlines (and as a result MIPAS detections) that match the AIRS cloud in terms of location and $SO_2$ concentration. This then allows us to mask out the clouds from the Grimsvotn eruption and highlight the clouds that likely originated from Nabro as seen in Figure 6.

## 3 Including AIRS Data into the Visualization (Task 3)

Viewing the data in the "2D" projected view allows users to visually compare the shape of AIRS clouds with the shape of the reconstructed MIPAS clouds that were derived from Task 2. Users can specify a threshold value for filtering detections in the AIRS dataset. The filtered result removes a large number of low intensity detections while enhancing regions of interest where ash and $SO_2$ are in relatively high concentration. This enables a clean comparison of these two data modalities without the interference of clean air detections. By superimposing the rendering results from both data sets and adjusting the time window, users have a large flexibility in assessing how well the two data agree with one another.

At first glance, we see that the major difference between the two data sets is that the reconstructed MIPAS cloud has a larger area of presence than the AIRS cloud. While the thresholding operation has some effect on this, this is mainly due to the fact that MIPAS is much more sensitive to lower particle concentrations than AIRS. With this in mind, we do observe that the shape of the clouds agree well with one another. For example, on June 7$^{th}$, the ash cloud from the Puyehue-Cordón Caulle eruption made a sharp turn to the north over the South Atlantic

Ocean. This was captured in both data sets as shown in Figure 7a. However, there are also some discrepancies. On June 21st , a slew of AIRS ash clouds turn northeast, overwhelming the city of Adelaide, Australia whereas the reconstructed MIPAS cloud evolution indicates that they wouldn't bend north until reaching the Tasman Sea (between Australia and New Zealand) as shown in Figure 7b.

We can also utilize discrepancies between the AIRS and MIPAS datasets to eliminate mineral dust clouds captured by the AIRS satellite. After projecting MIPAS detections onto the surface of the earth, we remove any AIRS points over the Sahara desert that only lie close to clean air MIPAS detections. This is because the MIPAS dataset is not sensitive to these mineral dust clouds.

One of the main disadvantages of using the AIRS dataset is that there is no altitude information associated with each detection. However, we can utilize the altitude information found in the CLaMS data to estimate the vertical extent of a particular AIRS measurement. This is done by clamping both AIRS and CLaMS data in a 12-hour time window, and projecting trajectories down onto the ground so that they lie on the same plane as the AIRS detections. Each AIRS point is then mapped to the closest CLaMS pathline and inherits the associating altitude information. This allows us to add a previously unavailable height estimate and additional temporal information to each AIRS detection. Users have the option to start the mapping in any 12-hour time window and then trace the mapped AIRS detections along the corresponding CLaMS trajectories to create a 3D time-varying visualization of the AIRS dataset as shown in Figure 8. This also gives users a good estimate of what the AIRS data could look like in the regions containing no data.

## 4 Air Traffic Response to Eruptions (Task 4)

To identify the effect of the eruptions on air traffic, we begin by identifying dangerous corridors which contain the highest concentration of dangerous substances. This is done by thresholding AIRS measurements that lie above a user-defined threshold. These detections are then correlated against MIPAS detections in a manner similar to Task 3. This allows us to classify the MIPAS points into several different groups using a parallel dbscan clustering algorithm [1] based on their latitude, longitude, and altitude information. Each point group is then constructed into a 3D convex polytope using the CGAL library [2] representing a potentially dangerous corridor.

To visualize the impact of the volcanic eruption, we utilize data from the flightstats website [3] containing over 3 million historical flight schedules as well as whether they were on time, delayed, or canceled. We focus on airports in the southern hemisphere over the same temporal span available in the volcanic datasets. Each flight is represented as a colored arc connecting the departure and arrival airports. Green arcs represent normally scheduled flights and red arcs represent flights that were either canceled or delayed. The extent of the delay is encoded into the saturation of the color with a higher saturation indicating a longer delay. A fully red path indicates that the flight was cancelled entirely. We also animate a specular highlight on each curve so that users can identify the direction of travel. Figure 9 shows flight data that lies within a 24 hour time window.

Animating the ash clouds as well as the flight data reveals many interesting observations. For example, we can see that flights in Chile were not interrupted initially since the wind was travelling from West to East. However, this wind caused the ash cloud to head towards Buenos Aires, grounding a large number of flights as seen in Figure 10a. Next, the subtropical jet stream carried the ash cloud all the way to Australia. Figure 10b shows that major cancellations are present and are consistent with the ash cloud's arrival. After the cloud completes its first circle around the globe it arrives in Chile again as seen in Figure 10c. This time, a large number of Chilean flights become canceled.

Moreover, looking at the raw MIPAS detection data superimposed onto the reconstructed MIPAS/AIRS cloud shows that there are ash detections present in certain locations even when there are no ash clouds present in the AIRS data because it is less sensitive to lower concentrations. One such instance occurs on June 15th between Australia and New Zealand. However, these low concentrations are still enough to ground flights between these two countries.

## 5 Aerosol Transport into the Statosphere (Task 5)

Lastly, we study how $SO_2$ from the Nabro eruption made its way into the stratosphere. Since there is currently a controversial discussion over the exact mechanism, we can use the various data modalities to contribute evidence towards this debate. We start by correlating both the CLaMS and MIPAS datasets with the associated tropopause altitude data and observing their spatial relationship over time.

We render the tropopause altitude data as a terrain map, where the height of the terrain is proportional to the tropopause boundary. The color helps to identify altitude variations with blue indicating a low altitude and yellow indicating a high altitude. An image of this terrain map can be seen in Figure 11. We ensure the same height scaling as used in rendering the CLaMS/MIPAS data to keep consistency when comparing the modalities. In this case, we show the CLaMS/MIPAS data in the same three hour time intervals that exist in the tropopause data. Any trajectories or points that lie below the tropopause become occluded by the terrain, making it easy to identify where they first appear and cross this boundary. Focusing around June 16th, while the Nabro volcano was erupting, one immediately notices CLaMS trajectories above the tropopause near the Nabro volcano itself as seen in Figure 11. However, this does not necessarily indicate that $SO_2$ from the Nabro eruption itself underwent vertical transport.

Another aspect of interest is the potential temperature and vorticity data along each CLaMS pathline. We allows users to select a region of interest and display the associated data for all pathlines in that region on a linked 2D plot (data vs. time) as seen in Figure 12. Any pathlines that have large gradients in the data have a steep slope in this plot. Users can also select interesting pathlines from this 2D window highlighting them in the 3D rendering as well. We can see that the majority of the trajectories that lie near the Nabro eruption event do not experience rapid changes in potential temperature. This can suggest that little to no vertical transport occurred after the eruption.

## References


[1] Mostofa Ali Patwary, Diana Palsetia, Ankit Agrawal, Wei-keng Liao, Fredrik Manne, and Alok Choudhary. A new scalable parallel DBSCAN algorithm using the disjoint-set data structure. *In Proceedings of the International Conference on High Performance Computing, Networking, Storage and Analysis (SC '12),* Article 62, 2012.

[2] Computational Geometry Algorithms Library (CGAL), [Online] 1998, http://www.cgal.org (Accessed May 2014).

[3] Flightstats Inc., [Online] 2012, http://www.flightstats.com (Accessed May 2014).

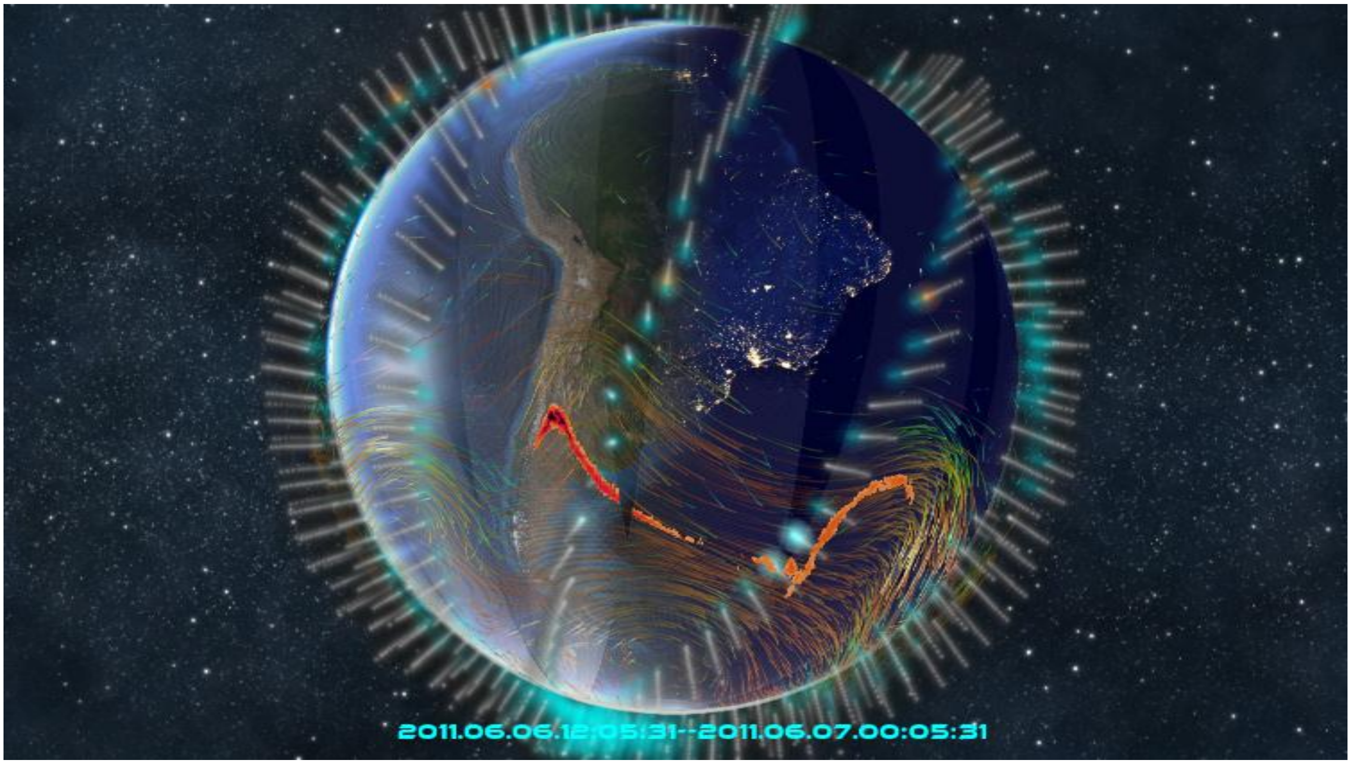


Figure 1: A view of the spherical representation of the earth with MIPAS point data, CLaMS pathlines, and AIRS detections simultaneously visible in the Southern Hemisphere.

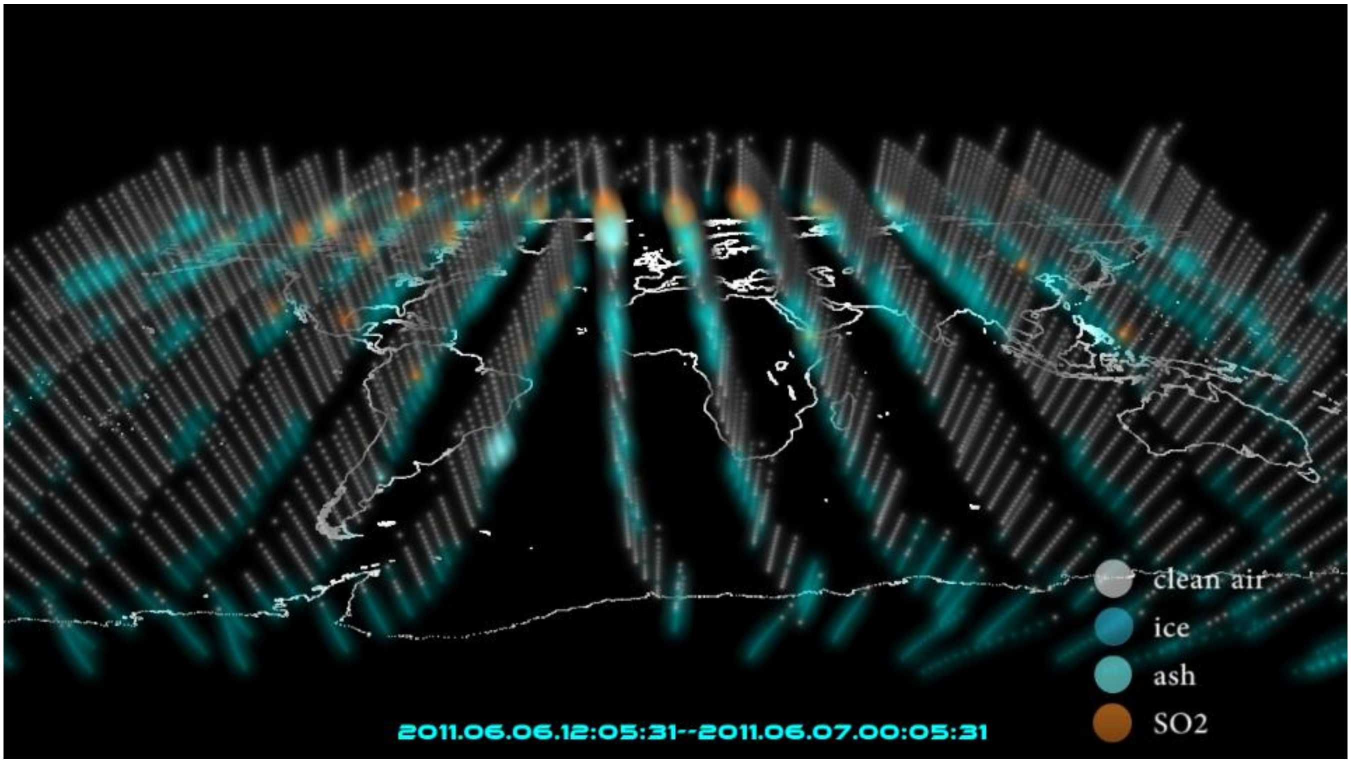


Figure 2: An overview of the MIPAS point data shown in the equirectangular projection view. Different colors are assigned to represent the type of detection.

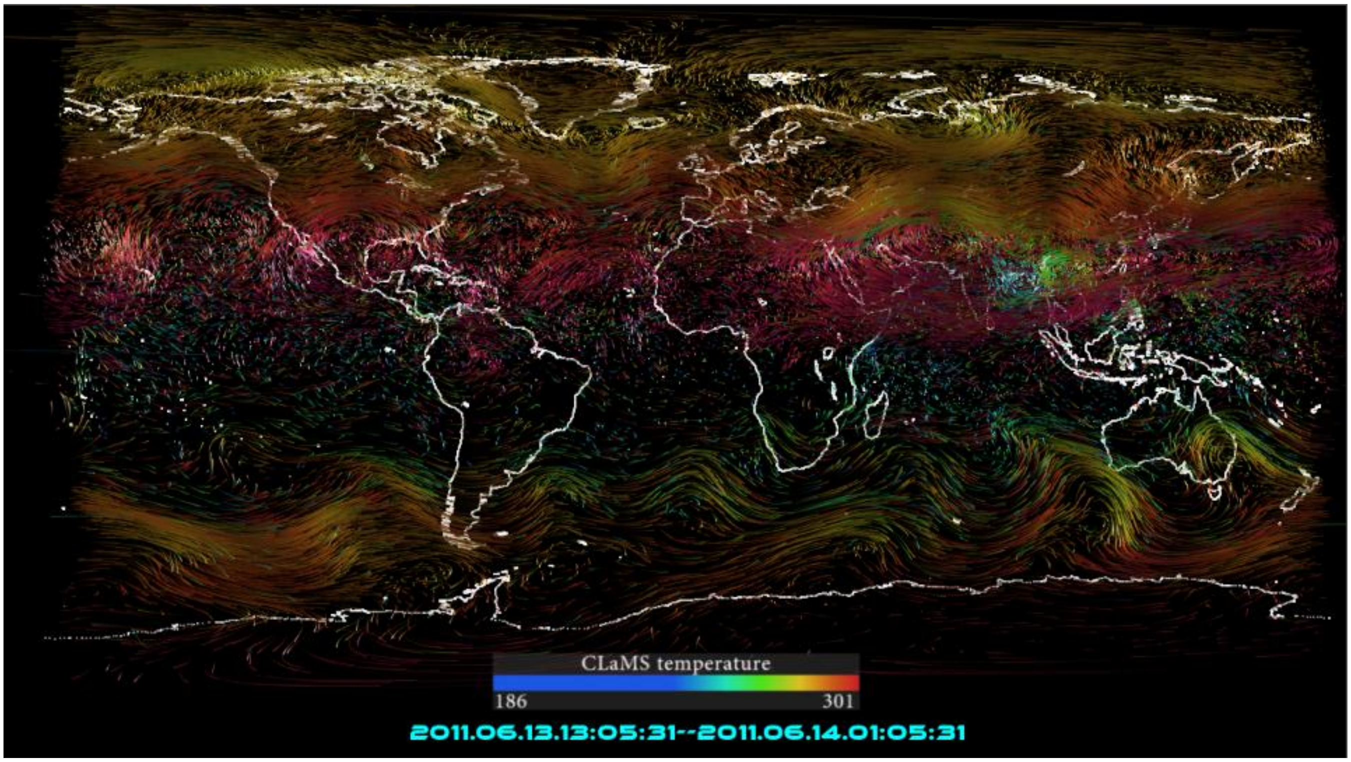


Figure 3: An overview of the CLaMS trajectory data colored according to temperature.

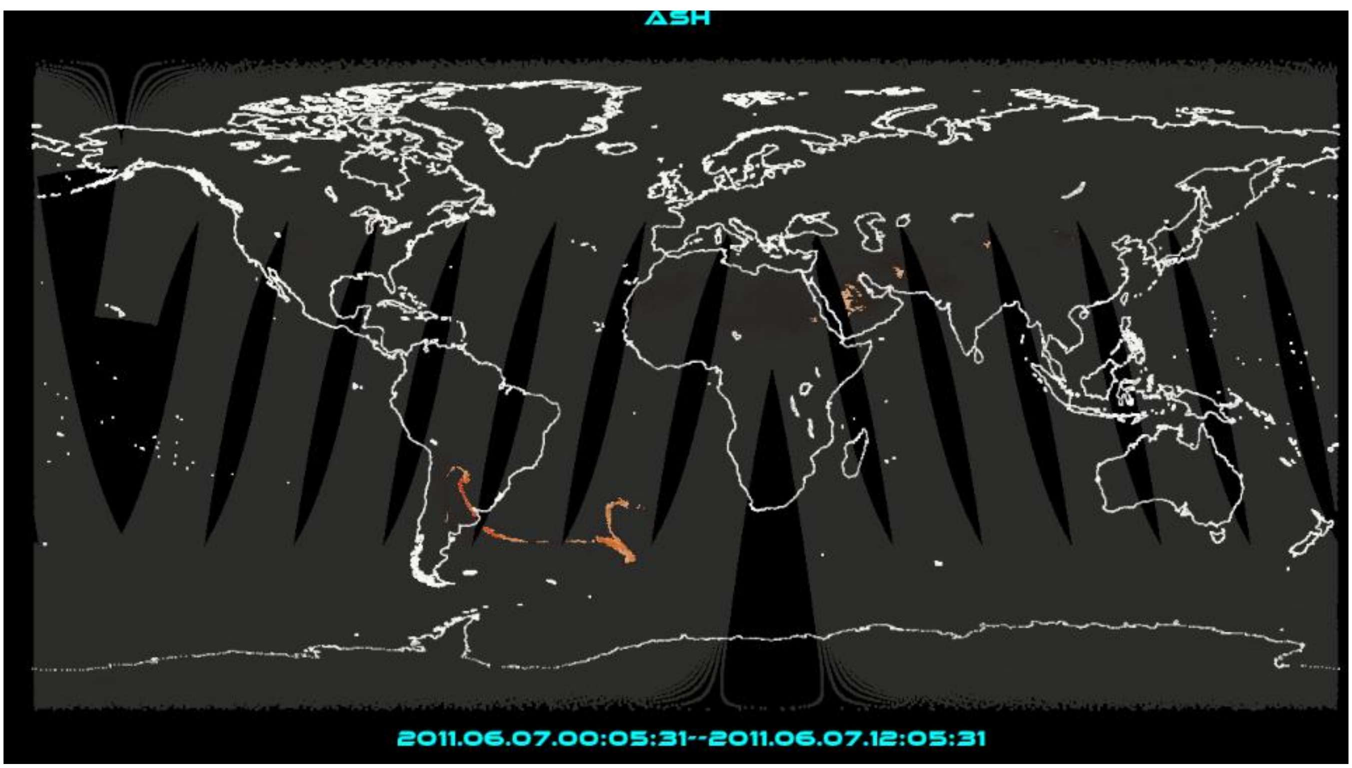


Figure 4: An image of the AIRS dataset with high ash concentrations shown in orange.

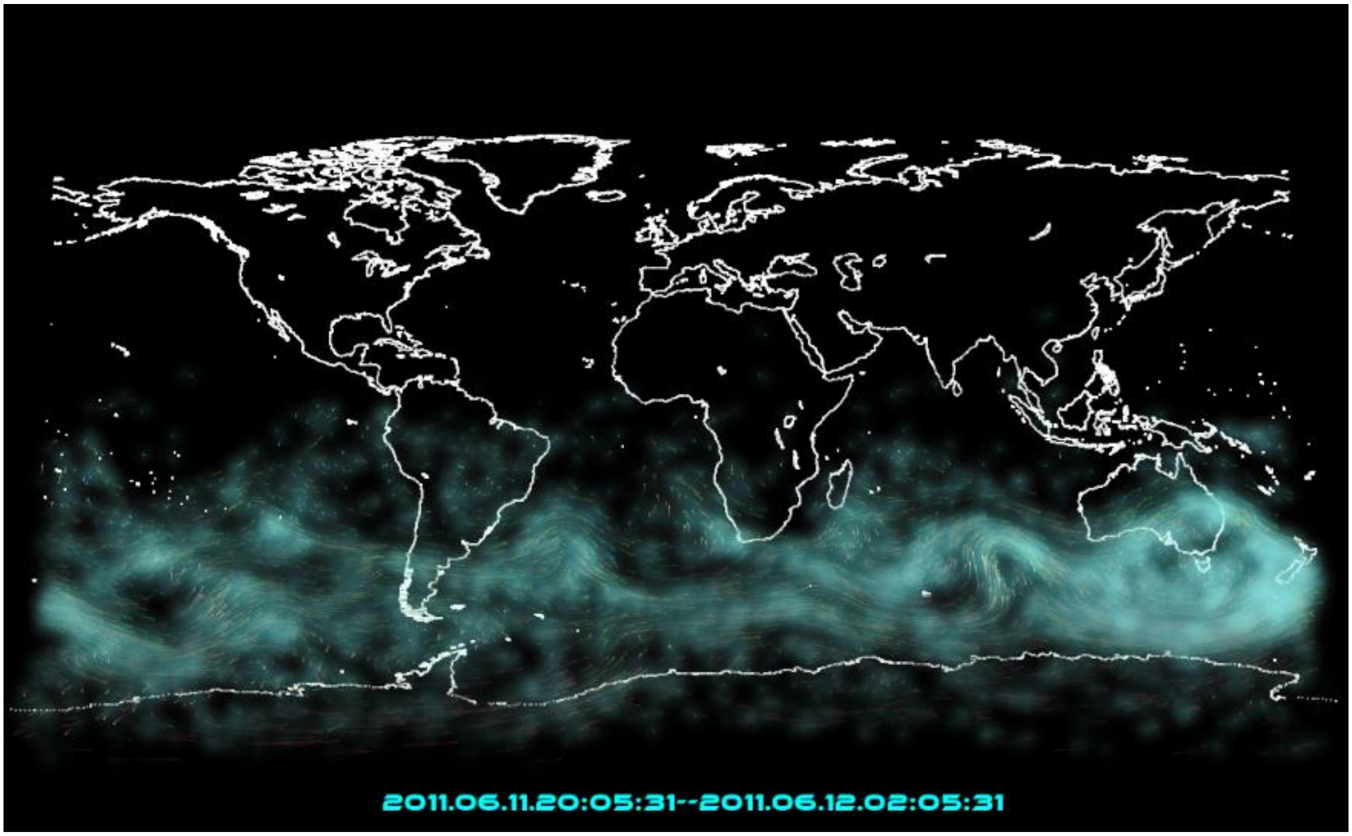


Figure 5: An overview of the reconstructed MIPAS/CLaMS cloud in the southern hemisphere overlaid onto the original CLaMS trajectories.

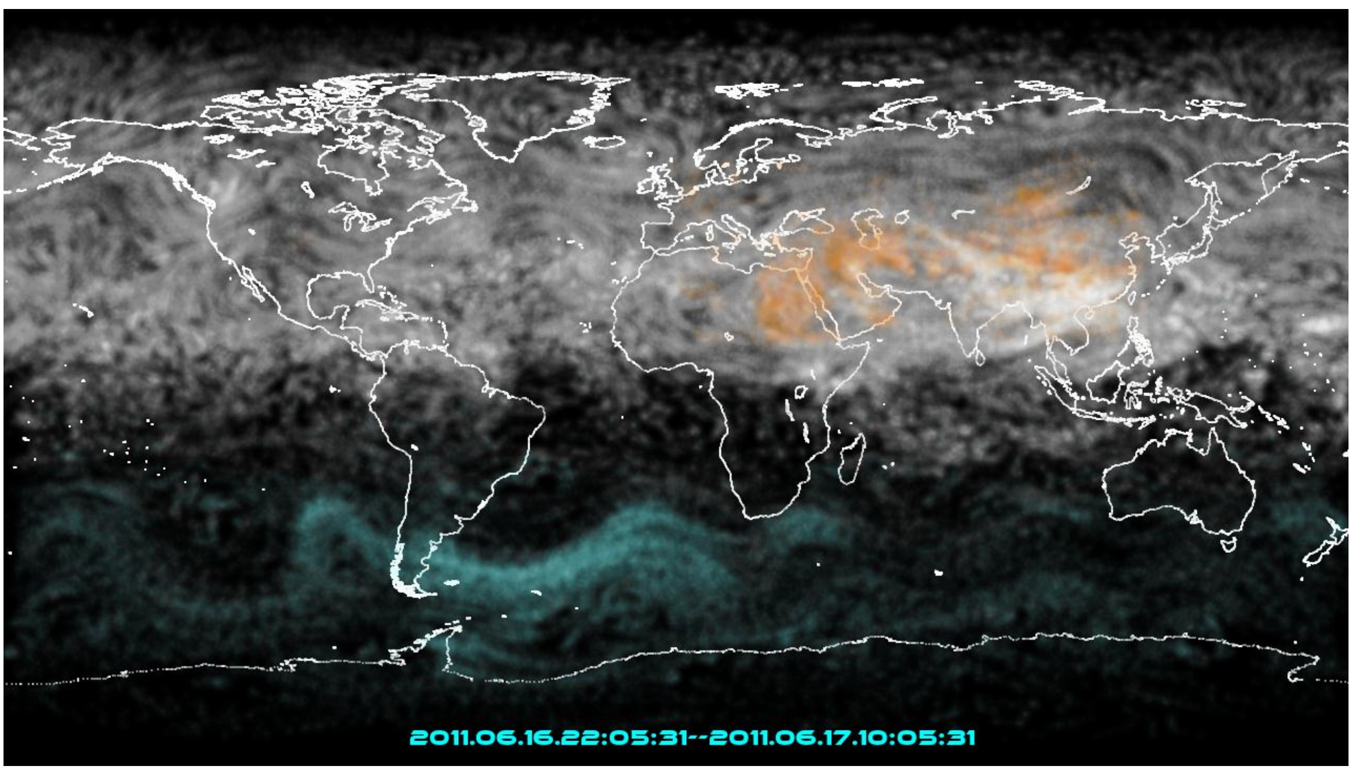


Figure 6: Associating the reconstructed MIPAS/CLaMS clouds with eruption events. The cloud generated using the southern hemisphere CLaMS trajectories is shown in teal. The cloud that likely originated from the Nabro eruption is shown in orange.

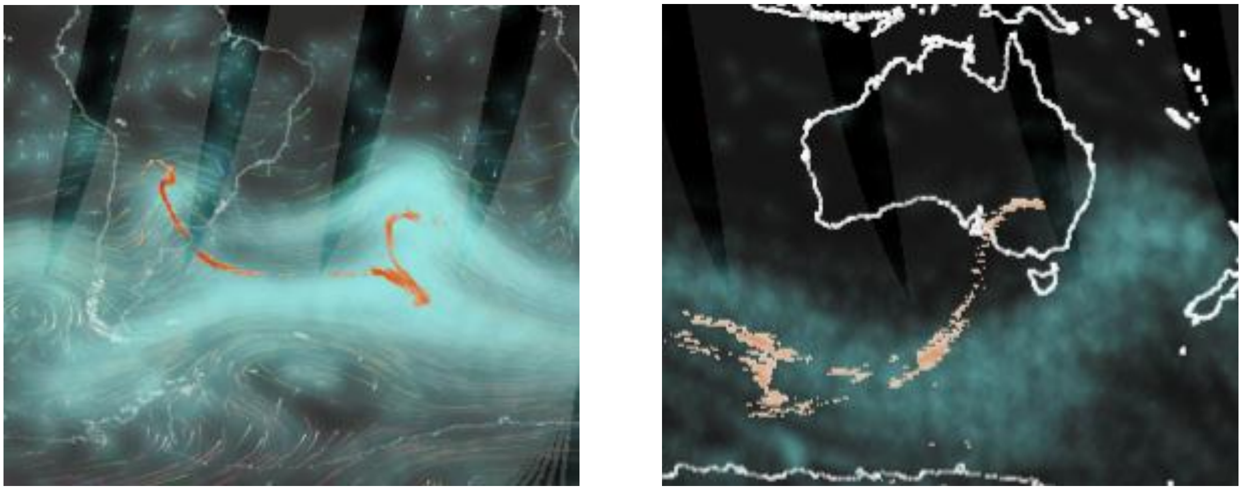

(a) June 7th (b) June 21st

Figure 7: (a) An image of June 7th showing how the shape of the AIRS and reconstructed MIPAS ash clouds agree although only high intensity detections are present in the less sensitive AIRS measurements. (b) An image of June 21st showing how the AIRS and reconstructed MIPAS ash clouds disagree.

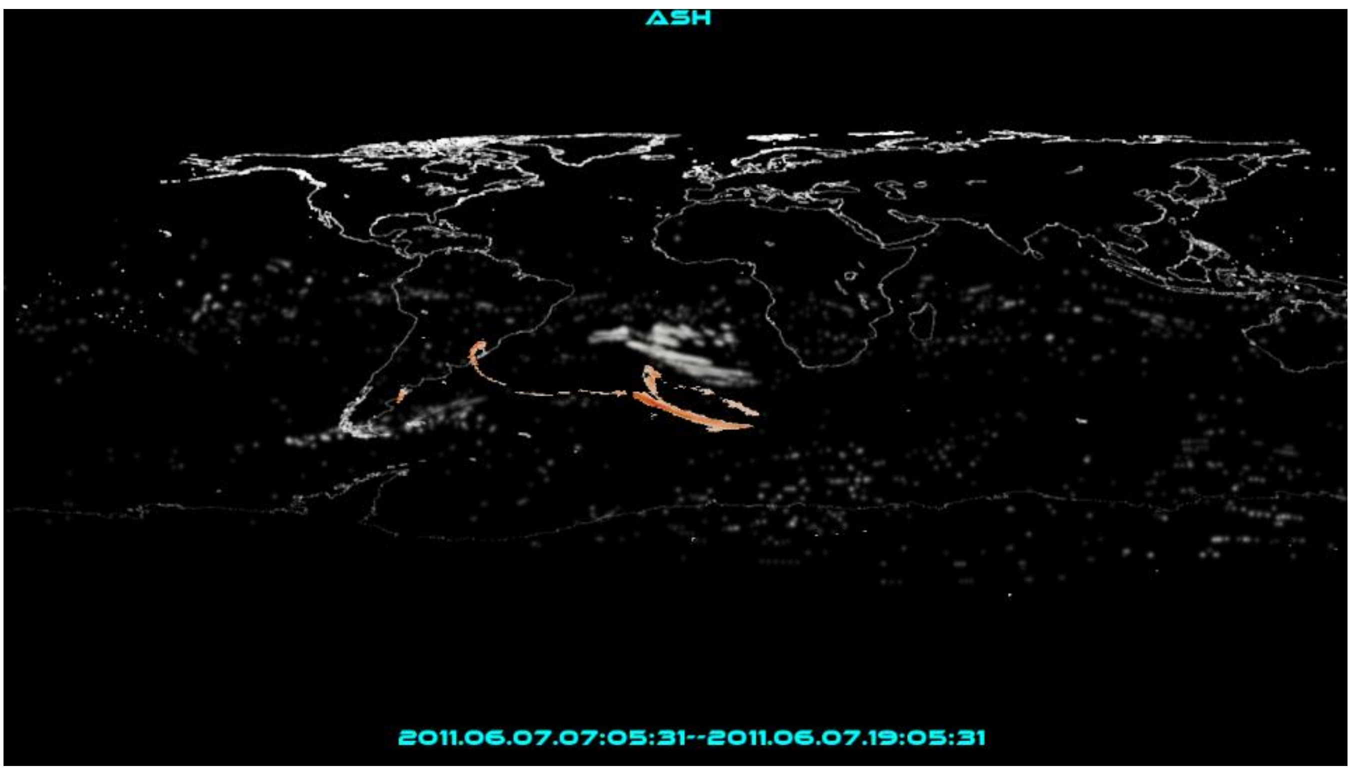


Figure 8: An angled view of the equirectangular projection with the original AIRS data (orange). The 3D reconstruction of the AIRS dataset (white) adds extra temporal information as well as a previously unavailable altitude estimate.

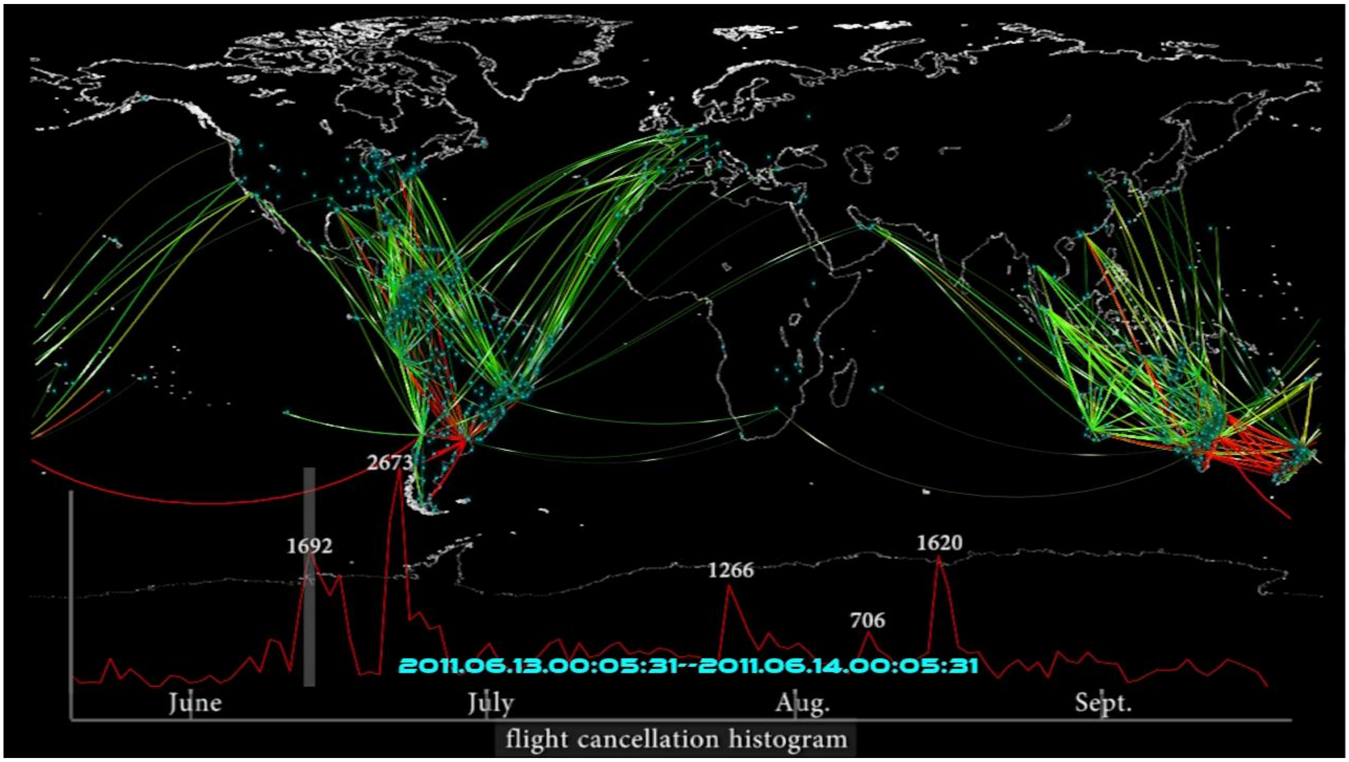


Figure 9: An overview of the flight schedule data over a 24 hour time window. Colored arcs represent a scheduled flight with source and destination airports represented as points. A line graph on the bottom of the visualization represents the number of affected flights over time.

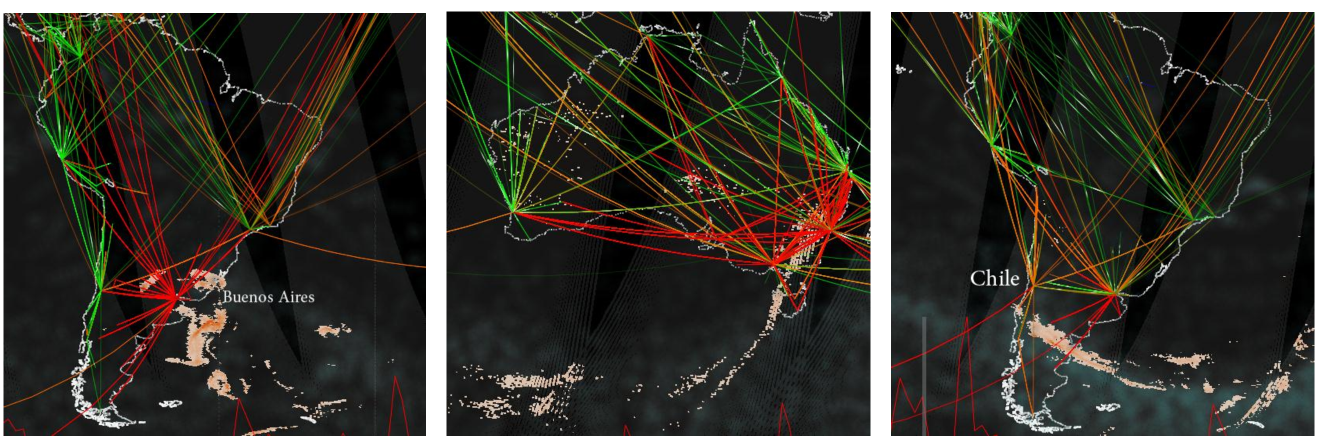


(a) Argentina (b) Australia (c) Chile

Figure 10: (a) The ash cloud first heads towards Argentina, grounding flights in Buenos Aires. Chile remains unaffected initially due to the wind direction. (b) The ash cloud travels to Australia affecting many flights as it arrives. (c) The cloud completes its first circle around the planet arriving in South America once again. This time many flights in Chile become affected.

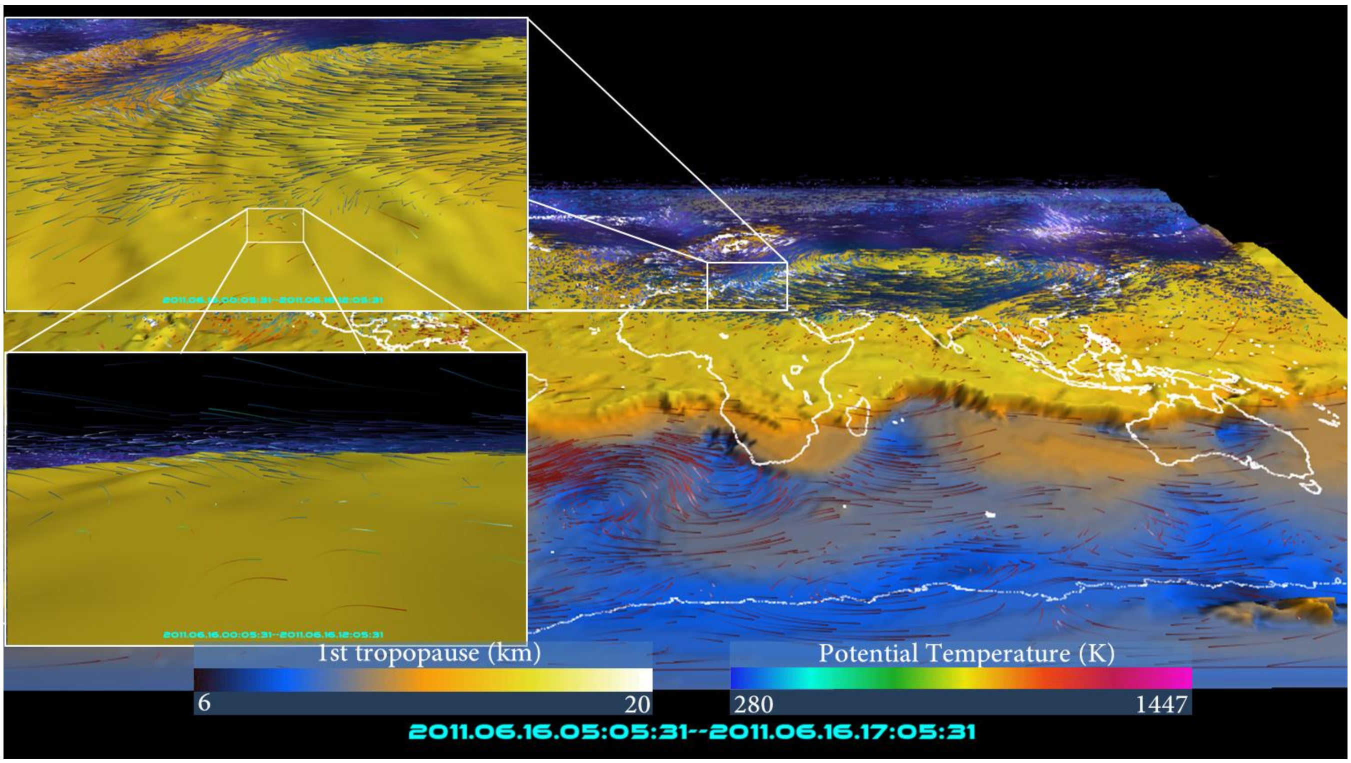


Figure 11: An image showing the tropopause dataset as a colored terrain map. Blue indicates lower altitudes while yellow indicates higher altitudes. CLaMS trajectories are colored according to potential temperature. Any trajectories that lie below the tropopause become occluded by the terrain, making it easy to identify where they first appear and cross this boundary.

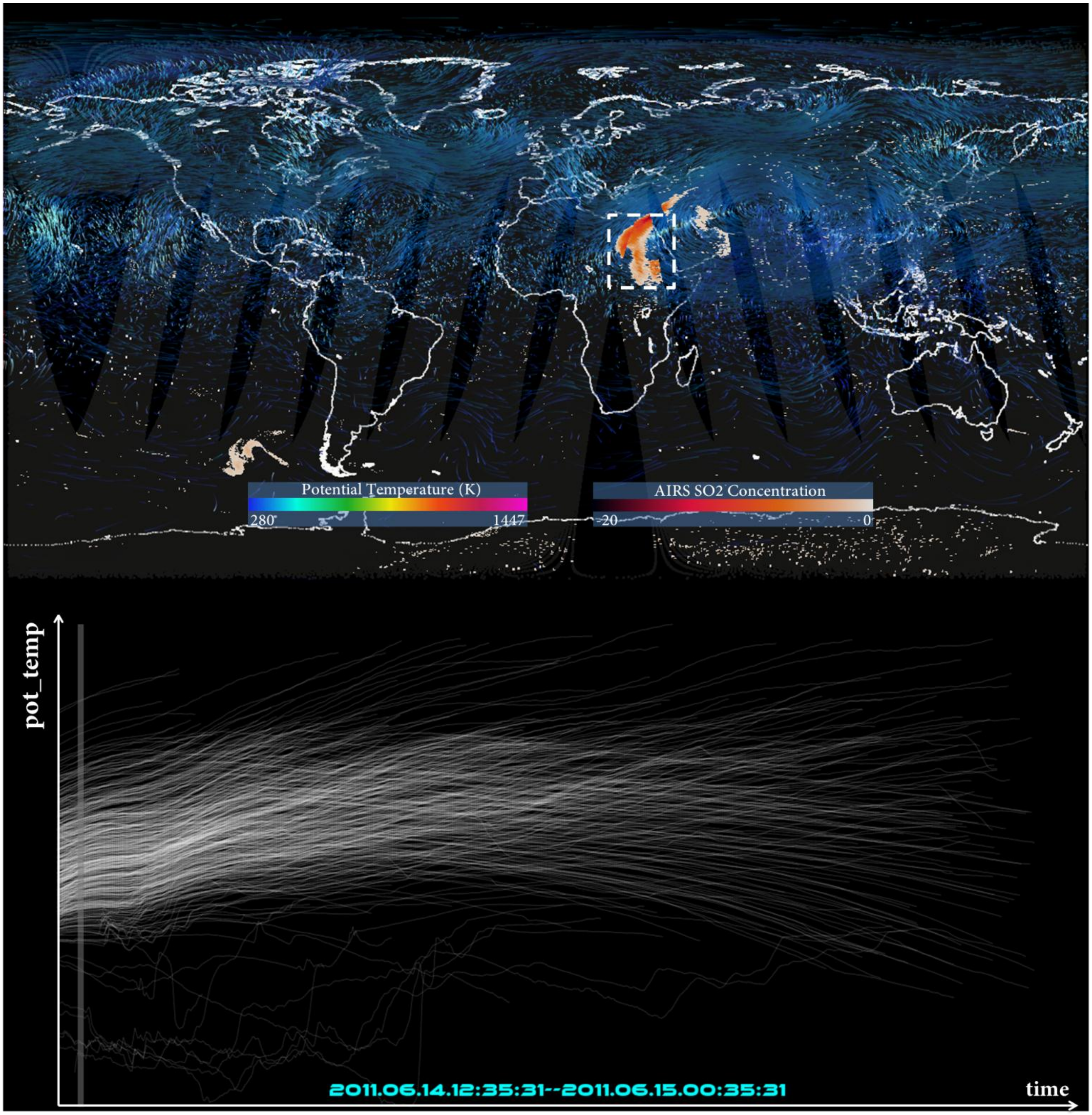


Figure 12: An image showing CLaMS trajectories colored according to potential temperature at the top of the screen. The corresponding data for the selected region around the Nabro eruption is plotted on the 2D graph at the bottom of the screen.